

Super-Poissonian Squeezed Light in the Ground State of Strongly Coupled Light-matter Systems

Cankut Tasçi,^{1,2} Mohammad Hassan,^{1,2} Leon Orlov-Sullivan,¹ Leonardo A. Cunha,³ and Johannes Flick^{1,2,3,*}

¹*Department of Physics, City College of New York, New York, NY 10031, USA*

²*Department of Physics, The Graduate Center, City University of New York, New York, NY 10016, USA*

³*Center for Computational Quantum Physics, Flatiron Institute, New York, 10010 NY, USA*

(Dated: December 23, 2025)

Strong light-matter coupling enables hybrid states in which photonic and electronic degrees of freedom become correlated even in the ground state. While many-body effects in long-range dispersion interactions are known to reshape electronic properties under such conditions, their impact on quantum-optical observables remains largely unexplored. Here, we address this problem using quantum electrodynamical density-functional theory (QEDFT) combined with the recently developed photon-many-body dispersion (pMBD) functional, which can capture higher-order electron-photon correlations and multi-photon processes. We compute ground-state photonic observables including photon number fluctuations, second-order correlations, and quadrature variances, and find squeezing and super-Poissonian photon statistics emerging from light-matter interactions in the strong coupling regime. Our results demonstrate that capturing the full hierarchy of many-body, electron-photon and multi-photon correlations is essential for a consistent description of quantum-optical properties in strongly coupled molecular systems, establishing QEDFT as a first-principles framework for predicting nonclassical photonic features in the ground state of complex systems.

Introduction: The emergence of strong light-matter interactions has opened new frontiers in chemistry and materials science [1]. In the strong coupling regime, when molecular or solid-state systems are embedded in optical or plasmonic cavities, matter excitations can hybridize with quantized electromagnetic modes, leading to novel chemical and physical properties. Particularly, the collective strong-coupling regime, where many molecules couple simultaneously to a cavity mode, has been the focus of numerous experimental efforts [2–5]. Recent studies [6–9] have demonstrated cavity-induced modifications of scaling relations in long-range dispersion and van der Waals interactions. In this regime, higher-order effects of the light-matter interaction can be expected to become important, as many-body effects are known to be essential already for electronic dispersion interactions [10].

A complementary perspective on strongly coupled light-matter systems arises from quantum optics and cavity QED, where the statistical properties of the field serve as sensitive probes of the underlying light-matter interaction [11, 12]. Quantities such as the photon-number distribution ($\langle \hat{a}^\dagger \hat{a} \rangle$), second-order correlations ($\langle \hat{a}^\dagger \hat{a}^\dagger \hat{a} \hat{a} \rangle$), and quadrature variances ($\langle \hat{q}^2 \rangle, \langle \hat{p}^2 \rangle$) capture the emergence of collective effects and non-classical coherence. These observables become relevant in phenomena such as superfluorescence and superradiance [13, 14], photon antibunching in single-emitter systems [15, 16], and the generation of squeezed vacuum states [17, 18]. To understand how macroscopic collective coupling modifies these signatures in molecular systems, a balanced treatment of quantum electrodynamics and electronic structure is necessary.

One approach for studying strongly coupled light-matter systems is quantum electrodynamical density-

functional theory (QEDFT). QEDFT provides an *ab initio* framework for coupled electron-photon systems, treating electronic and photonic degrees of freedom on equal footing [19, 20]. However, most applications of QEDFT to date have focused primarily on studying changes in the electronic structure, while the explicit treatment of quantum-optical observables, in particular collective coupling and many-photon effects, remains limited. This past focus can be primarily explained by limitations of existing exchange-correlation (xc) functionals currently available within QEDFT [21–26]. Many approximations neglect higher-order and multi-photon excitations, which are expected to be important in the collective strong-coupling regime. The absence of xc functionals capable of capturing these effects has restricted the predictive power of QEDFT, particularly for quantum-optical signatures.

In this work, we present an application of the photon many-body dispersion (pMBD) functional [9] to overcome these limitations and analyze ground-state quantum-optical observables for general light-matter coupled systems. The pMBD functional extends the original MBD framework [27–29] to systems under strong light-matter coupling and incorporates long-range many-body correlation effects between matter and quantized electromagnetic fields, thus enabling an accurate description of higher-order electron-photon processes that naturally arise in the collective regime. Because pMBD is explicitly many-body in both the electronic and photonic sectors, it allows these higher-order correlations to manifest directly in quantum-optical observables. Moreover, the pMBD formalism is constructed in a way that provides straightforward access to quantized photonic operators [30], including \hat{a} and \hat{a}^\dagger , making possible the eval-

uation of quantum-optical quantities and multi-photon correlation functions within an *ab initio* framework.

Theory: Due to the gauge freedom in quantum electrodynamics, the light-matter Hamiltonian may be expressed in different but physically equivalent representations. While the original pMBD Hamiltonian was formulated in the length gauge [9], in this work we reformulate the pMBD formulism in the velocity gauge to simplify the calculation of photonic observables. In the velocity gauge, the operators \hat{a}_α and \hat{a}_α^\dagger directly correspond to degrees of freedom of the cavity mode [31]. We refer to the SI for the transformation from length to velocity gauge.

In the velocity gauge, the pMBD Hamiltonian for a non-relativistic system of N_a atoms, and N_p quantized photon modes under dipole approximation then reads as

$$\begin{aligned} \hat{H} = & \frac{1}{2} \sum_{i=1}^{N_a} \sum_{a=1}^3 \left(i \hat{\nabla}_{ia} + \sum_{\alpha=1}^{N_p} \lambda_{\alpha a} \hat{q}_\alpha \sqrt{\alpha_{ia}} \omega_{ia} \right)^2 + \omega_{ia}^2 \chi_{ia}^2 \\ & + \frac{1}{2} \sum_{i,j=1}^{N_a} \sum_{a,b=1}^3 \omega_{ia} \omega_{jb} \sqrt{\alpha_{ia} \alpha_{jb}} \chi_{ia} T_{\text{LR},ij}^{ab} \chi_{jb} \\ & + \frac{1}{2} \sum_{\alpha=1}^{N_p} \hat{p}_\alpha^2 + \omega_\alpha^2 \hat{q}_\alpha^2, \end{aligned} \quad (1)$$

where $\chi_{ia} = \sqrt{m_i} \xi_{ia}$ describe the mass-weighted atomic displacements with effective atomic frequencies ω_{ia} , charges e_i , and polarizabilities $\alpha_{ia} = e_i^2/(m_i \omega_{ia}^2)$ [32]. $T_{\text{LR},ij}^{ab}$ is interaction tensor that describes the long-range dipole-dipole interaction between the individual atoms [33]. In the velocity gauge, the light-matter interaction is introduced via the coupling of the atomic momentum $i \hat{\nabla}_{ia}$ and the product of charge e_i and vector potential $\lambda_{\alpha a} \hat{q}_\alpha$.

The velocity-gauge Hamiltonian in Eq. 1 contains now coupling between position and momentum degrees of freedom, requiring the diagonalization of a $2(3N_a + N_p) \times 2(3N_a + N_p)$ matrix. We follow the procedure of Ref. 34, which correctly accounts for the commutation relations between momentum and position operators (see SI for details). This scaling is slightly different from the length-gauge formulation, where the position and momentum degrees of freedom formally become decoupled. As a consequence, the eigenvalues for the length-gauge pMBD Hamiltonian can be obtained by diagonalizing a $(3N_a + N_p) \times (3N_a + N_p)$ matrix. We note that instead of diagonalizing the pMBD Hamiltonian in Eq. 1 directly, the pMBD energy can be equivalently obtained as an integral over the imaginary frequency, which allows for a many-body order-by-order expansion of the energy.

Beyond providing the total exchange-correlation energy [9], the pMBD framework can be developed to access to a wide range of quantum-optical observables.

Second Quantization: To compute quantum-optical observables, it is both natural and advantageous to refor-

mulate the pMBD Hamiltonian in a second-quantized framework. This formalism provides a transparent and compact way to describe collective excitations, enabling the use of operator algebra to directly access photonic observables. Here, we follow the procedure outlined in Ref. 30 and, adapt it to the velocity gauge by following Ref. 34. We begin with the pMBD Hamiltonian in Eq. 1 expressed in terms of mass-weighted coordinates (χ_{ia}, q_α) and their corresponding momenta. A bosonic representation is then introduced via canonical quantization, where all atomic and photonic degrees of freedom are mapped to ladder operators. In a first step in Eq. 1, all position χ_{ia} and q_α operators and their conjugated momenta are replaced by (bosonic) creation and annihilation operators. In the next step, these original (bare) ladder operators are connected to the diagonalized collective normal modes \hat{b}, \hat{b}^\dagger through a Bogoliubov transformation:

$$\begin{pmatrix} \hat{b} \\ \hat{b}^\dagger \end{pmatrix} = \begin{pmatrix} X & Y \\ Y & X \end{pmatrix} \begin{pmatrix} \hat{a} \\ \hat{a}^\dagger \end{pmatrix}.$$

The transformation matrices X and Y capture the hybridization between photonic and electronic modes, providing direct insight into vacuum fluctuations and correlation effects. The precise definitions of the X and Y matrices, along with detailed derivations and proofs of the transformation formulas, are provided in the SI.

Having developed this connection now allows us to formulate various quantum-mechanical observables directly within the pMBD framework. For a given photon mode α with frequency ω_α , the quadrature variances $\langle \hat{q}_\alpha^2 \rangle$ and $\langle \hat{p}_\alpha^2 \rangle$ in terms of the Bogoliubov matrices X and Y are given by

$$\begin{aligned} \langle \hat{q}_\alpha^2 \rangle &= \frac{1}{\omega_\alpha} \left[(Y^T Y)_{\alpha,\alpha} - (X^T Y)_{\alpha,\alpha} + \frac{1}{2} \right], \\ \langle \hat{p}_\alpha^2 \rangle &= \omega_\alpha \left[(Y^T Y)_{\alpha,\alpha} + (X^T Y)_{\alpha,\alpha} + \frac{1}{2} \right]. \end{aligned}$$

Because the pMBD Hamiltonian in Eq. 1 is a quadratic Hamiltonian, its ground state is a zero-mean Gaussian state [35] where all first moments of the position and momentum operators (i.e. $\langle \chi_{ia} \rangle = \langle \hat{q}_\alpha \rangle = 0$) vanish. Consequently, all uncertainties reduce to $\Delta q_\alpha = \sqrt{\langle \hat{q}_\alpha^2 \rangle}$ and $\Delta p_\alpha = \sqrt{\langle \hat{p}_\alpha^2 \rangle}$. These uncertainties encode the complete Gaussian statistics of the dressed photon mode α , and therefore provide a direct handle on how light-matter coupling and many-body electronic correlations modify the quantum fluctuations of the electromagnetic field. In particular, deviations of $(\Delta q_\alpha, \Delta p_\alpha)$ from their vacuum values quantify the degree of squeezing induced by collective electronic response and photon hybridization. To quantify this squeezing, we calculate the squeezing parameter r_α of mode α , which can be written as [36]

$$r_\alpha = \frac{1}{2} \ln \left(\frac{\Delta q_\alpha}{\Delta p_\alpha / \omega_\alpha} \right) = \frac{1}{4} \ln \left(\frac{\langle \hat{q}_\alpha^2 \rangle \omega_\alpha}{\langle \hat{p}_\alpha^2 \rangle / \omega_\alpha} \right). \quad (2)$$

This formula makes it explicit that the effective squeezing arises from the renormalized quadrature variances $\langle \hat{q}_\alpha^2 \rangle$ and $\langle \hat{p}_\alpha^2 \rangle$ generated by the Bogoliubov coefficients (X, Y) . Importantly, this squeezing is not imposed externally but emerges from higher-order polarization effects and the light-matter dressing of the ground state, providing a direct link between electronic correlations and nonclassical photon statistics. The corresponding photon number is then given by the following equation

$$\langle \hat{n}_\alpha \rangle = \frac{\omega_\alpha \langle \hat{q}_\alpha^2 \rangle + \frac{1}{\omega_\alpha} \langle \hat{p}_\alpha^2 \rangle - 1}{2} = (Y^T Y)_{\alpha, \alpha}, \quad (3)$$

which quantifies the virtual photon population generated by strong light-matter coupling. The photon number has previously been analyzed within optimized-effective-potential (OEP) approaches [21] and can also be estimated using the photon-GA functional [23]. However, these earlier exchange-correlation approximations incorporate only first-order photon-mediated corrections and therefore can be expected to break down when higher-order light-matter correlations or multi-photon processes become important. In contrast, the pMBD functional includes the full hierarchy of higher-order mixed electron-photon contributions, enabling us to systematically assess how these effects modify the exchange-correlation energy, virtual photon populations, and nonclassical photon statistics in strongly coupled systems. Furthermore, the second-order photon correlation function $\langle \hat{a}_\alpha^\dagger \hat{a}_\alpha^\dagger \hat{a}_\alpha \hat{a}_\alpha \rangle$, which is central for quantifying photon statistics and the Mandel Q parameter [37], is defined as

$$\langle \hat{a}_\alpha^\dagger \hat{a}_\alpha^\dagger \hat{a}_\alpha \hat{a}_\alpha \rangle = 2(Y^T Y)_{\alpha, \alpha}^2 + (X^T Y)_{\alpha, \alpha}^2.$$

From these quantities, the Mandel Q parameter follows directly as

$$Q_\alpha = \frac{(Y^T Y)_{\alpha, \alpha}^2 + (X^T Y)_{\alpha, \alpha}^2}{(Y^T Y)_{\alpha, \alpha}}, \quad (4)$$

highlighting how photon-number fluctuations and higher-order light-matter correlations are encoded in the Bogoliubov coefficients. The Mandel Q parameter provides a simple way to distinguish photon statistics [38]: $Q < 0$ indicates sub-Poissonian (antibunched) light, $Q = 0$ corresponds to Poissonian (coherent) light, and $Q > 0$ reflects super-Poissonian behavior typically found in thermal or chaotic classical sources.

Finally, to quantify the entanglement between the cavity mode and the collective electronic excitations, we compute the Von Neumann entropy of the photonic subsystem, $S_{vN} = -\text{Tr}(\hat{\rho}_\alpha \ln \hat{\rho}_\alpha)$. Since the pMBD ground state is a Gaussian state, the reduced density matrix of the cavity mode $\hat{\rho}_\alpha$ is fully characterized by its covariance matrix [35, 39]. The entropy is determined solely by the symplectic eigenvalue ν_α of this covariance matrix,

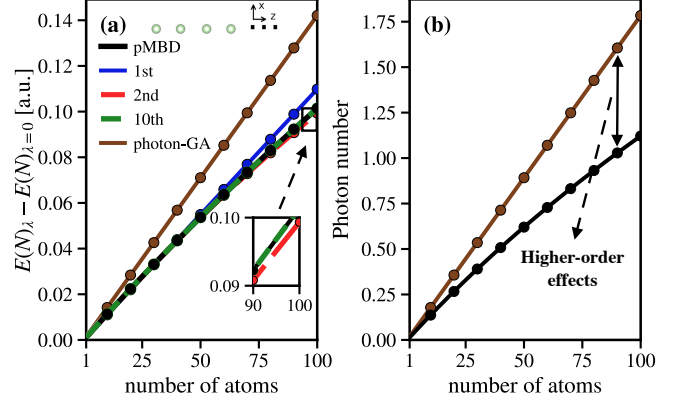


FIG. 1. Electron-photon exchange-correlation energy and photon number for chains of Ar atoms. (a) Electron-photon exchange-correlation energy predicted by pMBD (black), photon-GA (brown), and pMBD up to first (blue), second (red), and tenth order (green). The inset shows deviations between the second order and tenth/full pMBD results for a large number of atoms (90-100). In (b), we compare the ground-state photon number of pMBD (black) and photon-GA (brown).

which, given the absence of $x\text{-}p$ correlations in the diagonalized frame, is defined by the uncertainty product $\nu_\alpha = 2\sqrt{\langle \Delta \hat{q}_\alpha^2 \rangle \langle \Delta \hat{p}_\alpha^2 \rangle}$. The Von Neumann entropy is then given by [30]

$$S_{vN} = \frac{\nu_\alpha + 1}{2} \ln \left(\frac{\nu_\alpha + 1}{2} \right) - \frac{\nu_\alpha - 1}{2} \ln \left(\frac{\nu_\alpha - 1}{2} \right). \quad (5)$$

For a pure, non-entangled state (such as the vacuum state), the Heisenberg limit is saturated ($\nu_\alpha = 1$), yielding $S_{vN} = 0$. Values of $\nu_\alpha > 1$ (and thus $S_{vN} > 0$) indicate that the cavity mode is in a mixed state due to intrinsic entanglement with the electronic degrees of freedom.

Application: In the following, we apply the developed framework to one-dimensional chains of Ar atoms with a varying number of Ar atoms. These atoms are aligned in the z-axis, collectively coupled to a single cavity mode with polarization in the z-direction. For all results shown in this work, we apply a photon frequency of $\omega_\alpha = 2$ eV, a distance between Ar atoms of $d = 4$ Å and a light-matter coupling strength of $\lambda_\alpha = 0.025$ a.u. This geometry allows us to isolate how collective coupling modifies the ground-state energy, virtual photon population, and nonclassical photon statistics as the system size increases.

Fig. 1 illustrates the scaling behavior of the electron-photon interaction energy and the virtual photon population $\langle \hat{n}_\alpha \rangle$ (Eq. 3) as a function of system size for a linear chain of Ar atoms in an optical cavity as shown schematically in the figure. Specifically, Fig. 1(a) plots the difference in energy between coupled and uncoupled, $E(N)_\lambda - E(N)_{\lambda=0}$, as a function of the number of atoms N . The data compares the full pMBD result (black dash-

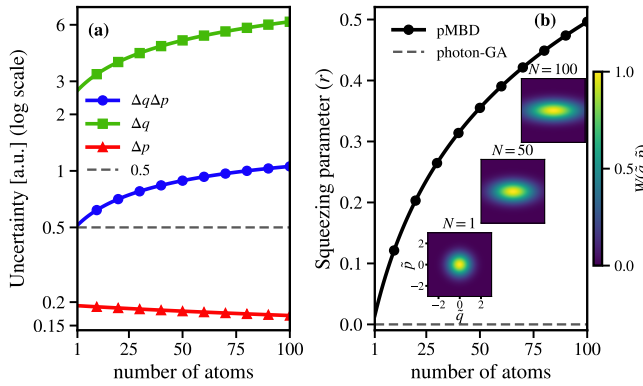


FIG. 2. Uncertainties and squeezing parameters for chains of Ar atoms. (a) Cavity quadrature uncertainties Δq (green squares) and Δp (red triangles), and their uncertainty product $\Delta q \Delta p$ (blue circles), as a function of the number of atoms N . The gray dashed line marks the Heisenberg uncertainty limit (0.5). (b) The squeezing parameter r predicted by pMBD (black circles), whereas the photon-GA functional (gray dashed line) predicts no squeezing ($r = 0$). Insets display the Wigner quasiprobability distributions $W(\tilde{q}, \tilde{p})$ in dimensionless phase-space coordinates ($\tilde{q} = \omega_\alpha q$, $\tilde{p} = p/\omega_\alpha$) for $N = 1$, 50, and 100, visualizing the phase-space deformation predicted by pMBD.

dotted line) with the photon-GA functional (brown line with circles) and various orders of the pMBD many-body expansion: 1st order (blue solid line), 2nd order (red solid line), and 10th order (green dashed line) using the order-by-order expansion via frequency-integration. The inset provides a magnified view of the large- N limit ($N = 90$ to 100). From Fig. 1(a), we see that both the first-order approximation and the photon-GA functional scale linearly with the number of atoms N [22]. In contrast, the second and higher orders progressively converge toward the full pMBD result, which exhibits a sublinear growth. Using the pMBD functional, we find that, as N increases, higher-order processes lead to a deviation of accumulating energy additively [40], resulting in a reduced effective contribution per atom that simple single-photon functionals, such as the photon GA functional, cannot capture. Fig. 1(b) displays the corresponding total photon number as a function of the number of atoms N , explicitly contrasting the photon-GA prediction (brown) with the pMBD result (black). While the photon-GA functional predicts a linear increase of $\langle \hat{n}_\alpha \rangle$ with system size again, the pMBD result grows more slowly and displays a clear sublinear trend. This difference further highlights the collective nature of the interaction: as more atoms couple to the cavity, higher-order effects redistribute the virtual photon population, deviating from the linear prediction of independent-particle models.

Fig. 2 characterizes the quantum statistical properties of the cavity mode as a function of the number of atoms N . Fig. 2(a) plots the quadrature uncertainties predicted by pMBD: the position uncertainty Δq_α

(green squares), the momentum uncertainty Δp_α (red triangles), and their Heisenberg product $\Delta q_\alpha \Delta p_\alpha$ (blue circles). The theoretical vacuum limit of 0.5 [41] is indicated by the grey dashed line for reference. From Fig. 2(a), we see how collective light-matter interactions reshape the quantum fluctuations of the cavity mode. As the number of atoms N increases, the quadrature uncertainties diverge from the vacuum level: the state becomes increasingly squeezed in the p -quadrature while expanding in the q -quadrature. Similar features were observed in Ref. [42] for an increase in λ_α instead of the number of atoms N . Fig. 2(b) displays the squeezing parameter r (Eq. 2) calculated via the pMBD method (red circles) compared to the photon-GA prediction (grey dashed line), which remains zero. The insets in Fig. 2(b) visualize the corresponding Wigner distributions of the cavity photon state in the pMBD framework at three distinct system sizes ($N = 1$, 50, and 100), illustrating the deformation of the state's fluctuations in phase space. This phase-space deformation is highlighted by the Wigner distributions, which stretch from a vacuum circle into an elongated ellipse as N increases. This visualizes the quantitative trend of the squeezing parameter r , confirming that the reduction in momentum uncertainty corresponds to a coherent squeezing of the vacuum state, despite the overall increase in the uncertainty product.

Finally, Fig. 3 characterizes the quantum nature of the cavity fluctuations by analyzing the photon statistics. Fig. 3(a) displays the Mandel Q parameter (Eq. 4) (blue squares) and the photon number variance Δn_α^2 (red circles) as a function of the number of atoms N . The results from the pMBD method (solid lines) are contrasted with the photon-GA approximation (dashed lines). The dotted grey line at $Q = 0$ represents the Poissonian limit characteristic of coherent states; values below this line ($Q < 0$) indicate sub-Poissonian statistics, while values above ($Q > 0$) indicate super-Poissonian behavior. Here, pMBD predicts strongly super-Poissonian statistics with $Q > 2$ for $N = 100$ with significant values as well in the photon number variance Δn_α^2 . In contrast, the photon-GA method (dashed lines) predicts sub-Poissonian statistics ($Q < 0$). However, this is not a physical signature of quantum antibunching, but rather a failure of the approximation. Since the photon-GA method includes only single-photon processes, the two-photon correlation function vanishes ($\langle \hat{a}_\alpha^\dagger \hat{a}_\alpha^\dagger \hat{a}_\alpha \hat{a}_\alpha \rangle = 0$). Consequently, the photon number variance is artificially truncated to $\Delta n_\alpha^2 = \langle \hat{n}_\alpha^2 \rangle - \langle \hat{n}_\alpha \rangle^2$, forcing the Mandel parameter to be negative ($Q = -\langle \hat{n}_\alpha \rangle$). Thus, the observed sub-Poissonian statistics arise from an incorrect truncation of the two-photon Hilbert space, rather than a genuine quantum origin. Fig. 3(b) investigates the nature of the fluctuations by plotting the von Neumann entropy S_{VN} (Eq. 5) against the mean photon number. The pMBD results (black diamonds) are compared to the photon-GA predictions (red circles) and the theo-

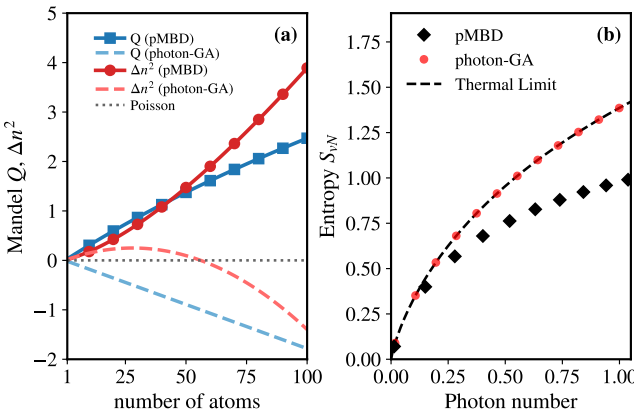


FIG. 3. Entanglement and correlations for chains of Ar atoms. (a) Mandel Q parameter (blue squares) and photon number variance Δn^2 (red circles). The gray dotted line marks the Poissonian limit ($Q = 0$). (b) Von Neumann entanglement entropy S_{vN} vs photon number. The pMBD (black diamonds) predicts less entropy than the thermal limit (dashed black line), whereas the photon-GA (red circles) predicts a thermal-like behavior.

retical thermal limit (black dashed line), which represents the maximum entropy for a given photon number. In contrast to photon-GA in Fig. 3 (a), pMBD predicts a physical transition to super-Poissonian statistics ($Q > 0$). While such broadened distributions are often associated with signatures of classical thermal noise, Fig. 3(b) rules out thermalization as the cause. The pMBD entropy reveals a significant deviation from a thermal distribution, as the entropy values are significantly below the thermal limit. This gap demonstrates that the super-Poissonian statistics observed in Fig. 3(a) are not driven by thermal mixing, but rather by the squeezed vacuum nature of the state. As the phase space ellipse stretches (see Fig. 2), it intersects higher photon number states, creating large number fluctuations ($\Delta n_\alpha^2 > \langle \hat{n}_\alpha \rangle$) while maintaining the low entropy of a pure quantum state. This observation of super-Poissonian squeezed light aligns with recent analytical solutions of the deep-strong-coupling Quantum Rabi Model [36]. We also note that a squeezed wave function ansatz has been recently successfully used for QED Hartree-Fock [43].

Conclusion: In summary, we have introduced a framework for computing photonic observables in strongly coupled light-matter systems within the pMBD framework of QEDFT. This approach captures collective, higher-order, and multi-photon processes that emerge when many emitters interact with a single cavity mode. Applications to chains of Ar atoms demonstrate that collective coupling leads to sublinear photon number scaling and the emergence of non-classical photon statistics. These results show that many-body and multi-photon contributions are essential for a consistent description of both energetic and photonic properties, beyond the scope of

simpler functionals that truncate the photonic subspace.

Acknowledgments: We acknowledge funding from the Defense Advanced Research Projects Agency (DARPA), and startup funding from the City College of New York. The Flatiron Institute is a division of the Simons Foundation.

* Electronic address: jflick@ccny.cuny.org

- [1] F. J. Garcia-Vidal, C. Ciuti, and T. W. Ebbesen, Manipulating matter by strong coupling to vacuum fields, *Science* **373**, eabd0336 (2021).
- [2] A. Thomas, L. Lethuillier-Karl, K. Nagarajan, R. M. A. Vergauwe, J. George, T. Chervy, A. Shalabney, E. Devaux, C. Genet, J. Moran, and T. W. Ebbesen, Tilting a ground-state reactivity landscape by vibrational strong coupling, *Science* **363**, 615 (2019).
- [3] B. Xiang, R. F. Ribeiro, M. Du, L. Chen, Z. Yang, J. Wang, J. Yuen-Zhou, and W. Xiong, Intermolecular vibrational energy transfer enabled by microcavity strong light-matter coupling, *Science* **368**, 665 (2020).
- [4] W. Ahn, J. F. Triana, F. Recabal, F. Herrera, and B. S. Simpkins, Modification of ground-state chemical reactivity via light-matter coherence in infrared cavities, *Science* **380**, 1165 (2023).
- [5] B. Patrahan, M. Piejko, R. J. Mayer, C. Antheaume, T. Sangchai, G. Ragazzon, A. Jayachandran, E. Devaux, C. Genet, J. Moran, and T. W. Ebbesen, Direct observation of polaritonic chemistry by nuclear magnetic resonance spectroscopy, *Angewandte Chemie International Edition* **63**, e202401368 (2024).
- [6] T. S. Haugland, J. P. Philbin, T. K. Ghosh, M. Chen, H. Koch, and P. Narang, Understanding the polaritonic ground state in cavity quantum electrodynamics, *The Journal of Chemical Physics* **162**, 194106 (2025).
- [7] J. P. Philbin, T. S. Haugland, T. K. Ghosh, E. Ronca, M. Chen, P. Narang, and H. Koch, Molecular van der waals fluids in cavity quantum electrodynamics, *The Journal of Physical Chemistry Letters* **14**, 8988 (2023).
- [8] J. Cao and E. Pollak, Cavity-induced quantum interference and collective interactions in van der waals systems, *The Journal of Physical Chemistry Letters* **16**, 5466–5472 (2025).
- [9] C. Tasçi, L. A. Cunha, and J. Flick, Photon many-body dispersion: An exchange-correlation functional for strongly coupled light-matter systems, *Physical Review Letters* **134**, 073002 (2025).
- [10] A. G. Donchev, Many-body effects of dispersion interaction, *The Journal of Chemical Physics* **125**, 074713 (2006).
- [11] H. J. Carmichael, Photon antibunching and squeezing for a single atom in a resonant cavity, *Phys. Rev. Lett.* **55**, 2790 (1985).
- [12] G. Rempe, R. J. Thompson, R. J. Brecha, W. D. Lee, and H. J. Kimble, Optical bistability and photon statistics in cavity quantum electrodynamics, *Phys. Rev. Lett.* **67**, 1727 (1991).
- [13] R. G. DeVoe and R. G. Brewer, Observation of superradiant and subradiant spontaneous emission of two trapped ions, *Phys. Rev. Lett.* **76**, 2049 (1996).
- [14] T. Brandes, Coherent and collective quantum optical ef-

fects in mesoscopic systems, *Phys. Rep.* **408**, 315 (2005).

[15] T. Basché, W. E. Moerner, M. Orrit, and H. Tallet, Photon antibunching in the fluorescence of a single dye molecule trapped in a solid, *Phys. Rev. Lett.* **69**, 1516 (1992).

[16] P. Michler, A. Kiraz, C. Becher, W. V. Schoenfeld, P. M. Petroff, L. Zhang, E. Hu, and A. Imamoglu, A quantum dot single-photon turnstile device, *Science* **290**, 2282 (2000).

[17] G. Breitenbach, S. Schiller, and J. Mlynek, Measurement of the quantum states of squeezed light, *Nature* **387**, 471 (1997).

[18] E. S. Polzik, J. Carri, and H. J. Kimble, Spectroscopy with squeezed light, *Phys. Rev. Lett.* **68**, 3020 (1992).

[19] I. V. Tokatly, Time-dependent density functional theory for many-electron systems interacting with cavity photons, *Phys. Rev. Lett.* **110**, 233001 (2013).

[20] M. Ruggenthaler, J. Flick, C. Pellegrini, H. Appel, I. V. Tokatly, and A. Rubio, Quantum-electrodynamical density-functional theory: Bridging quantum optics and electronic-structure theory, *Phys. Rev. A* **90**, 012508 (2014).

[21] C. Pellegrini, J. Flick, I. V. Tokatly, H. Appel, and A. Rubio, Optimized effective potential for quantum electrodynamical time-dependent density functional theory, *Phys. Rev. Lett.* **115**, 093001 (2015).

[22] J. Flick, C. Schäfer, M. Ruggenthaler, H. Appel, and A. Rubio, Ab initio optimized effective potentials for real molecules in optical cavities: Photon contributions to the molecular ground state, *ACS Photonics* **5**, 992 (2018).

[23] J. Flick, Simple exchange-correlation energy functionals for strongly coupled light-matter systems based on the fluctuation-dissipation theorem, *Phys. Rev. Lett.* **129**, 143201 (2022).

[24] C. Schäfer, F. Buchholz, M. Penz, M. Ruggenthaler, and A. Rubio, Making ab initio qed functional(s): Nonperturbative and photon-free effective frameworks for strong light-matter coupling, *Proc. Natl. Acad. Sci. U.S.A.* **118**, e2110464118 (2021).

[25] I.-T. Lu, M. Ruggenthaler, N. Tancogne-Dejean, S. Lartini, M. Penz, and A. Rubio, Electron-photon exchange-correlation approximation for quantum-electrodynamical density-functional theory, *Physical Review A* **109**, 052823 (2024).

[26] D. Mejia-Rodriguez and N. Govind, A meta-generalized gradient approximation for the cavity-dependent exchange-correlation interaction in strongly coupled light-matter systems, *The Journal of Physical Chemistry Letters* **16**, 13139 (2025).

[27] A. Tkatchenko and M. Scheffler, Accurate molecular van der waals interactions from ground-state electron density and free-atom reference data, *Phys. Rev. Lett.* **102**, 073005 (2009).

[28] A. Tkatchenko, R. A. DiStasio, R. Car, and M. Scheffler, Accurate and efficient method for many-body van der waals interactions, *Phys. Rev. Lett.* **108**, 236402 (2012).

[29] A. Tkatchenko, A. Ambrosetti, and J. DiStasio, Robert A., Interatomic methods for the dispersion energy derived from the adiabatic connection fluctuation-dissipation theorem, *The Journal of Chemical Physics* **138**, 074106 (2013).

[30] M. Gori, P. Kurian, and A. Tkatchenko, Second quantization of many-body dispersion interactions for chemical and biological systems, *Nature Communications* **14**, 8218 (2023).

[31] C. Schäfer, M. Ruggenthaler, V. Rokaj, and A. Rubio, Relevance of the quadratic diamagnetic and self-polarization terms in cavity quantum electrodynamics, *ACS Photonics* **7**, 975 (2020), PMID: 32322607.

[32] We note that we follow regular procedure to obtain α_{ia} and related parameters via Hirshfeld decomposition and rsscs equations [28, 29].

[33] A. Ambrosetti, A. M. Reilly, J. DiStasio, Robert A., and A. Tkatchenko, Long-range correlation energy calculated from coupled atomic response functions, *The Journal of Chemical Physics* **140**, 18A508 (2014).

[34] J. Colpa, Diagonalization of the quadratic boson hamiltonian, *Physica A: Statistical Mechanics and its Applications* **93**, 327 (1978).

[35] C. Weedbrook, S. Pirandola, R. García-Patrón, N. J. Cerf, T. C. Ralph, J. H. Shapiro, and S. Lloyd, Gaussian quantum information, *Rev. Mod. Phys.* **84**, 621 (2012).

[36] C.-F. Kam and X. Hu, Super-poissonian squeezed light in the deep strong regime of the quantum rabi model, arXiv preprint 10.48550/arXiv.2412.04085 (2024).

[37] L. Mandel, Sub-poissonian photon statistics in resonance fluorescence, *Opt. Lett.* **4**, 205 (1979).

[38] L. Mandel and E. Wolf, *Optical Coherence and Quantum Optics* (Cambridge University Press, 1995).

[39] A. Serafini, *Quantum Continuous Variables: A Primer of Theoretical Methods* (CRC Press, Boca Raton, 2017).

[40] D. Novokreschenov, A. Kudlis, I. Iorsh, and I. V. Tokatly, Quantum electrodynamical density functional theory for generalized dicke model, *Phys. Rev. B* **108**, 235424 (2023).

[41] D. F. Walls, Squeezed states of light, *Nature* **306**, 141 (1983).

[42] Y. Tang, G. M. Andolina, A. Cuzzocrea, M. Mezera, P. B. Szabó, Z. Schätzle, F. Noé, and P. A. Erdman, Deep quantum monte carlo approach for polaritonic chemistry, *The Journal of Chemical Physics* **163**, 034108 (2025).

[43] I. M. Mazin and Y. Zhang, Light-matter hybridization and entanglement from first-principles, arXiv preprint arXiv:2411.15022 (2024).